CO2 Removal from a CO2–CH4 Gas Mixture by Clathrate Hydrate Formation Using THF and SDS as Water-Soluble Hydrate Promoters

Marvin Ricaurte, Christophe Dicharry, Daniel Broseta, Xavier Renaud, Jean-Philippe Torre

CO_2 Removal from a CO_2−CH_4 Gas Mixture by Clathrate Hydrate Formation Using THF and SDS as Water-Soluble Hydrate Promoters

Marvin Ricaurte,[†] Christophe Dicharry,[†] Daniel Broseta,[†] Xavier Renaud,[‡] and Jean-Philippe Torré*[,†]

[†]CNRS, TOTAL−UMR 5150−LFC R−Laboratoire des Fluides Complexes et leurs Réservoirs, Université de Pau et des Pays de l'Adour, Avenue de l'Université, BP 1155, Pau, F 64013, France

[‡]Total, Centre Scientifique et Technique Jean Féger (CSTJF), Avenue Larribau, Pau, F 64018, France

ABSTRACT: This study investigates the use of hydrate formation to separate the CO_2 from a CO_2−CH_4 gas mixture in the presence of water soluble additives—tetrahydrofuran (THF) and/or sodium dodecyl sulfate (SDS)—at low concentrations. The influence of additive concentration and process operating conditions on the gas enclathration kinetics, the quantity of gas removed, and the selectivity of the separation are studied under quiescent hydrate forming conditions in a batch reactor. Gas consumption and enclathration occur at high rates only when the two additives are used in combination. Similarly to what has been observed with pure CO_2, the proposed mechanism is that a mixed hydrate of structure sII containing THF forms first, which triggers the formation of CO_2−CH_4 binary gas hydrate of structure sI. However, the gas separation was found not to be selective enough to the CO_2 for envisaging any practical application.

1. INTRODUCTION

Natural gas is important in various sectors of the economy, e.g., in electricity generation, industrial heat source and chemical feedstock, and water and space heating in residential and commercial buildings. In 2009, natural gas consumption in the world was close to 3 trillion m^3,[1] and regarding the huge quantity of potential reserves present on the globe, natural gas will continue to expand its relative importance in world energy markets.[2] Raw natural gas is generally a complex gaseous mixture containing mostly methane, and CO_2 is often one of the most important contaminants (with heavier hydrocarbons, aromatic and aliphatic compounds, water vapor, and other acid gases such as hydrogen sulfide). CO_2 is encountered in an increasing number of natural gas fields, where its content can reach and even exceed 50 vol %,[3] and it must be separated from the gas stream prior to commercialization. The presence of CO_2 in natural gas is not suitable as it decreases its calorific value, can be responsible for blockage in process equipment (e.g., cryogenic units), and can contribute, if water is present, to the corrosion of steel pipes during transport.

Most of the conventional processes available to remove CO_2 and other acid gases (such as H_2S) from natural gas streams are based on chemical absorption (using amines or carbonate solutions), physical absorption (using methanol or glycols), adsorption processes on solid sorbents (using molecular sieve adsorbents or activated carbons), hybrid absorption (using a combination of chemical and physical solvents), and physical separation (using membranes). These processes, extensively described in the literature,[4,5] have proven their effectiveness for the selective removal of CO_2, but their major drawback is their large energy costs.[6] Research efforts to enhance the efficiency of the current gas separation processes or to develop novel technologies are therefore necessary. As a contribution to these efforts, we have investigated a gas hydrate based process to separate CO_2 from a CO_2−CH_4 gas mixture rich in CO_2, which is reported in this paper.

Clathrate hydrates (called hydrates in the following) are nonstoichiometric icelike inclusion compounds formed, typically at moderately high pressure (a few megapascals) and low temperatures (a few degrees above 273 K), by combination of water ("host" molecules) and small molecules ("guest" molecules) such as nitrogen, methane, carbon dioxide, acetone, tetrahydrofuran, and cyclopentane.[7] Two hydrate structures, usually called "structure one" (denoted sI) and "structure two" (denoted sII), are generally encountered. Structure sI is a body centered cubic structure, formed by two small (5^{12}) and six large ($5^{12}6^2$) cavities, with 46 water molecules per unit cell: sI hydrates have the general formula $2(5^{12})\cdot6(5^{12}6^2)\cdot46H_2O$.[8] Structure sII is a diamond lattice within a cubic framework which contains two different types of cavities—a small one denoted (5^{12}) and a large one denoted ($5^{12}6^4$)—and 136 water molecules per unit cell: the general formula of sII hydrates is $16(5^{12})\cdot8(5^{12}6^4)\cdot136H_2O$.[8] Gas hydrates are of great scientific and/or economic interest, with various industrial applications[9] such as flow assurance,[10] gas storage and transportation, desalination, refrigeration and air conditioning, and gas separation processes.[11]

The separation of CO_2 by formation of clathrate hydrates has already been studied for various types of gas mixtures.[12] This technique is considered as a long term interesting option[13] and a promising technology,[14] potentially economically competitive[15] in comparison to the conventional processes, especially when the CO_2 is to be injected and stored in a geological formation. In this case, the compression costs needed for the injection could be considerably reduced, since the capture process is carried out at high pressure. However, the hydrate based process actually suffers from important limitations which

Received: September 23, 2012
Revised: November 30, 2012
Accepted: December 3, 2012
Published: December 3, 2012

dx.doi.org/10.1021/ie3025888

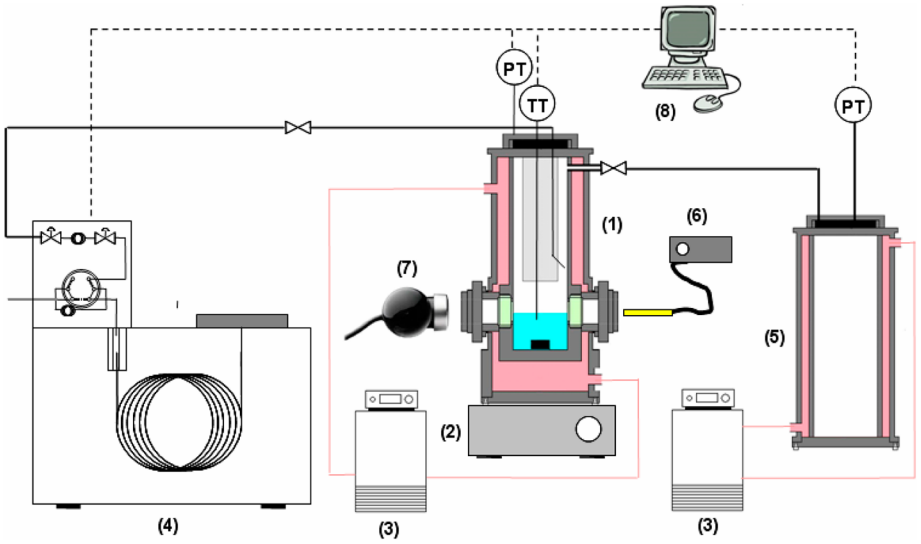

Figure 1. Schematic diagram of the experimental apparatus: (1) hydrate forming reactor; (2) magnetic agitator; (3) thermostatic baths; (4) high pressure gas chromatograph; (5) gas storage vessel; (6) lighting system; (7) video camera; (8) data acquisition system.

have prevented until now the deployment of this technology from laboratory to larger scale, such as the severe thermodynamic conditions necessary to form these structures in some cases, the low hydrate formation kinetics, and the insufficient selectivity toward CO_2. Some studies have reported that, under appropriate pressure and temperature conditions, hydrates formed from a CO_2−CH_4 gas mixture contain more than 90 mol % CO_2 when the equilibrium vapor phase composition is in the range of 40 mol % CO_2.[16,17] However, recent works[18,19] show that the proximity of the CO_2 and CH_4 hydrate phase boundaries renders very difficult their separation by means of hydrate crystallization, and the separation performance may be limited by the relatively small differences between the free energies for CO_2 and CH_4 in the hydrate cages.[4] On the other hand, it could be possible to imagine a "dynamic separation" between CO_2 and CH_4, in which the CO_2 uptake by gas hydrate formation proceeds initially more quickly than the methane uptake:[18,20] this interesting concept has been developed very recently, from a theoretical point of view, by Herri et al.[21]

One of the possibilities for unlocking some of the above limitations is to use chemical additives (water soluble or not) such as surfactants,[22] organic compounds,[23] polymers,[24] and quaternary ammonium salts.[25] Conventionally, these additives are classified as either kinetic or thermodynamic promoters. The latter, which typically consist of organic compounds such as cyclic ethers or quaternary ammonium salts, shift the equilibrium conditions toward higher temperatures or lower pressures. Kinetic additives (generally surfactant molecules) have the effect to accelerate hydrate formation without changing the hydrate equilibrium conditions. The action mechanism by which surfactants promote hydrate growth is still unclear and continues to be hardly debated.[26,27] In this study, we have chosen to investigate a combination of two very well known hydrate promoters: sodium dodecyl sulfate (SDS), which is an anionic surfactant, and tetrahydrofuran (THF), which is a cyclic ether. Interestingly, a small amount of SDS (a few tens to hundreds parts per million) added to the aqueous phase is known to increase drastically the kinetics of methane hydrate formation.[28,29] In addition, various studies[30,31] report that THF is able to reduce significantly the hydrate equilibrium pressure at a given temperature even at low dosage in the aqueous phase.[32] Finally, these two additives (SDS + THF) used simultaneously have already proven to perform well to enhance pure CO_2 hydrate formation (formation rate and amount of hydrate formed) at concentrations greater than 1500 ppm for SDS and ranging from 1.0 to 4.0 wt % for THF.[33,34] However, results concerning such a combination of additives have not been reported for hydrate formation from gas mixtures.

The objectives of the present work are to test this combination of additives (SDS + THF) on the separation of CO_2 by hydrate formation from a CO_2−CH_4 gas mixture rich in CO_2. In particular, we investigate the influence of the additive concentration, and the effects of the operating conditions (particularly the gas loading pressure and the hydrate formation temperature), on both the kinetics and the selectivity of CO_2 capture. The technical description of the experimental rig and the material used in this study are presented in section 2. Then, the experimental results obtained are detailed and discussed in section 3, where mechanisms by which the additives promote hydrate formation are proposed. Finally, the conclusions of this work are in section 4.

2. MATERIALS, EXPERIMENTAL RIG, AND KEY PARAMETERS

The additives used in this study are THF (purity > 99.9% from Sigma Aldrich) and SDS (purity > 98% from Chem Lab). Ultrapure water (resistivity of 18.2 MΩ·cm) produced by a laboratory water purification system from Purelab is used for preparing the aqueous solutions containing the additives. The CO_2−CH_4 gas mixture used in this work (gas supplied by Air Liquide) contains 75.02 ± 0.50 mol % CO_2 and 24.98 ± 0.50 mol % CH_4.

The pilot rig used for hydrate formation is depicted schematically in Figure 1. The hydrate forming reactor, connected to a gas storage vessel and a high pressure gas chromatograph, is a jacketed titanium cylindrical vessel (364.7 ± 0.9 cm^3 of internal volume), equipped with two see through sapphire windows of 20 mm diameter. Stirring is ensured by means of a star shaped magnetic agitator. The liquid and gas temperatures are measured with PT100 probes, and the reactor

pressure is measured with a 0−10 MPa pressure transducer, where the accuracies (integrating the data acquisition system and the repeatability of the measurements) are estimated to ±0.2 K and ±0.02 MPa, respectively. A standard PC equipped with a LabView interface allows recording the data with a frequency of 1 Hz. A CCD camera (Model OptiaII from Creative Laboratories) located in front of one of the two sapphire windows of the reactor allows visualizing the different hydrate morphologies during the experiment. A gas chromato graph (Agilent, Model GC6980), equipped with a capillary column (Model HP PLOT Q from Agilent) and a thermal conductivity detector (TCD), is connected to the reactor to perform gas composition analyses. The whole system is optimized to avoid pressure perturbations when the gas is sampled (sampling volume equal to 0.05 cm^3), and the resulting pressure drop for each gas analysis is considered negligible (less than 0.001 MPa). The precision of the analysis is less than 2.0 mol %, as evaluated through calibration measurements with different CO_2−CH_4 gas mixtures.

The experiments are carried out in a batch reactor, i.e., under isochoric conditions, meaning that after the reactor has been loaded with the aqueous solution and the gas, the system is isolated and the total quantity of matter present inside the reactor is a constant (the amount of gas removed by samplings is negligible). In this case, the molar quantity of matter removed from the gas phase by gas enclathration and/or solubilization into the solution, denoted $n_{removed}$, is calculated by mass balance using eq 1:

$$n^i_{removed} = n^i_g|_{t_{init}} - n^i_g|_{t_{final}} = \left.\frac{y^i PV}{zRT}\right|_{t_{init}} - \left.\frac{y^i PV}{zRT}\right|_{t_{final}} \quad (1)$$

where superscript i corresponds to the constituent (CO_2 or CH_4) present in the gas mixture, y^i is the molar composition of the constituent i in the mixture, z is the compressibility factor calculated using the Peng−Robinson equation of state (PR EoS), P is the reactor pressure, T is the reactor temperature, V is the volume of the gas phase, and t_{init} and t_{final} are the initial and final times of the experiment. The initial time t_{init} is the time when the reactor is loaded with the gas, and $t_{init} = 0$ in the following. During the initial reactor pressurization step (total duration time of about 2 min with agitator in the off position), we have estimated experimentally (pure CO_2 and a solution containing 4.0 wt % THF and 3000 ppm SDS, P_{init} = 4.00 MPa and T^R = 303 K) that the quantity of CO_2 dissolved in the solution was less than 0.5% of the total amount of the CO_2 present in the aqueous solution at the solubility equilibrium. Therefore, we have neglected the quantity of CO_2 dissolved (by diffusion) in the liquid phase during this period.

The selectivity of the separation (denoted S) quantifies the performance of the process to separate the CO_2 from the CO_2−CH_4 gas mixture. We define S as the ratio of the molar quantity of CO_2 removed from the gas phase to the molar quantity of the CH_4 removed from the gas phase:

$$S = \frac{n^{CO_2}_{removed}}{n^{CH_4}_{removed}} \quad (2)$$

Note that the quantities of THF and water present in the gas phase have been quantified in a previous study[34] and can be considered as negligible at the pressure and temperature conditions used here.

Two parameters, denoted $t_{50\%}$ and $t_{90\%}$, have been defined to compare the kinetics of hydrate formation obtained with the different experimental conditions tested here. The times $t_{50\%}$ and $t_{90\%}$ (expressed in minutes) are defined as the time necessary (from the beginning of the experiment) to reach respectively 50% and 90% of the total quantity of removed gas (in moles) obtained at the end of the experiment.

Finally, the parameter called the enclathration rate, denoted dn/dt and expressed in moles per minute, is calculated directly on the kinetic curve (molar quantity of gas removed versus time), and corresponds to the maximum value of the gas rate consumption. This value is obtained numerically by determi nation of the inflection point located on the kinetic curve.

3. RESULTS AND DISCUSSION

3.1. Detail of a Typical Experiment. Figure 2 shows the variation of the process parameters (reactor pressure and temperature), the gas composition, and the amount of gas removed from the reactor gas phase during a typical experiment carried out with the two additives used in combination. Visual observations (snapshots) are also presented together with the

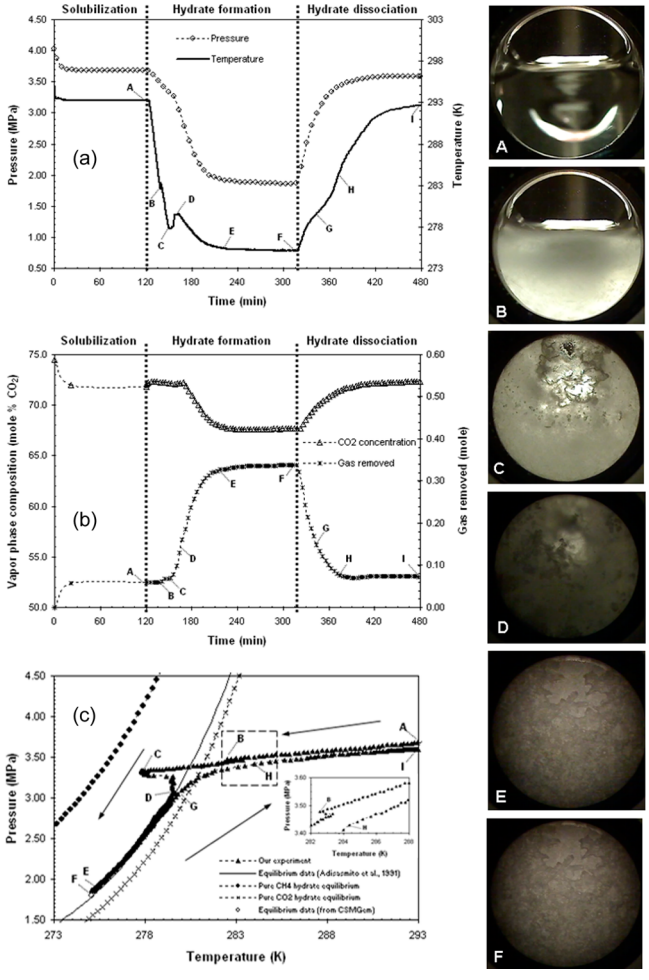

Figure 2. Typical curves and snapshots obtained during a hydrate formation and dissociation experiment: (a) reactor pressure and temperature versus time; (b) vapor phase composition and quantity of gas removed versus time; (c) pressure−temperature diagram, together with hydrate equilibrium data for CO_2−CH_4 gas mixture, pure CO_2, and pure CH_4. Conditions: [SDS] = 3000 ppm, [THF] = 4.0 wt %, T_{targ} = 275 K, and P_{load} = 4.00 MPa.

data. The concentrations of the two additives, THF and SDS, are here 4.0 wt % and 3000 ppm (by weight), respectively. Our observations are presented together with a discussion of the possible mechanisms.

3.1.1. Protocol. A quantity of 65.0 ± 0.1 cm^3 of solution is first introduced into the reactor. Then, the reactor is closed, connected to the rest of the rig, and purged two times with the CO_2−CH_4 gas mixture (agitator off). The initial reactor temperature is fixed to the value of T_{init} = 293 K, and the reactor pressure is adjusted to the desired value with the gas mixture (P_{load} = 4.00 MPa in this example). In this period (duration of 2 min), the agitator remains off. An analysis of the gas phase is always performed at this moment to obtain precisely the initial gas composition. The agitation is then started at 600 rpm and the solution is maintained under agitation at 293 K for 120 min for gas solubilization. Then, the reactor is cooled at 0.9 K/min from 293 K to the target temperature T_{targ}—which is always higher than the ice point (here T_{targ} = 275 K)—and is maintained constant for at least 180 min. Finally, at time t_{final}, the reactor temperature is raised back to 293 K at 1.5 K/min. During all the steps of this protocol, the gas phase is sampled every 3.40 min.

3.1.2. Observations. As shown in Figure 2a, the initial decrease in reactor pressure is essentially due to the CO_2 solubilization into the aqueous solution. Figure 2b shows a rapid decrease of the CO_2 concentration in the gas phase, and the CH_4 solubilization can be considered negligible as the two solubility values differ typically by a least 1 order of magnitude.[35] The solubility equilibrium is usually reached within 30 min, and the pressure in the reactor stabilizes to a constant value. In this example, the equilibrium pressure reached by the system and the CO_2 concentration in the gas phase are respectively equal to 3.69 MPa and 71.8 mol %, corresponding to a quantity of removed gas equal to 0.060 mol (9.8% of the gas loaded initially).

From point A to point B in Figure 2a, the reactor pressure drops because of the reactor cooling and the gas solubilization. At point B, a sudden increase of temperature is measured due to a first crystallization of hydrates in the bulk (shown in snapshot B). It is important to note that, as the magnetic agitator is not able to maintain a sufficient stirring of the slurry during the whole experiment, we have decided to stop it (manually) as soon as a crystallization is observed. Therefore, the events taking place after point B are occurring in quiescent conditions.

From point B to point C (see Figure 2a), the reactor pressure continues to decrease at a moderate rate, and at point C, a second crystallization is starting in the bulk, as manifested by a substantial increase of temperature (in the range of several kelvin), concomitant with a large quantity of solids generated in the bulk (as shown in snapshot C).

From point C to point E (see Figure 2a), a dramatic decrease in reactor pressure is measured, together with important modifications in the morphology of the hydrate formed (compare snapshots C and E), associated with a sharp decrease in CO_2 concentration in the gas phase (Figure 2b). Then, the reactor temperature and pressure and the gas phase composition begin to stabilize and constant values are finally reached. No substantial change is observed concerning the aspect of the solids visible from point E to point F (as shown by comparison of snapshots E and F in Figure 2). At point F, P^R = 1.86 MPa, T^R = 275 K, and y^{CO_2} = 67.7 mol %, and the quantity of removed gas is 0.338 mol, corresponding to 55.5% of the initial gas loaded into the reactor.

During the final temperature rise (from 275 to 293 K), two small "bumps" in the profile of the pressure vs time curve, are apparent (points G and H in Figure 2a), which could be attributed to the decomposition of the two types of hydrates formed previously. At the end of the experiment (point I), the reactor pressure stabilizes at a value very close to the pressure reached after the solubilization period (point A). The small difference, which is generally less than 0.09 MPa, results from the samplings of the gas during the experiment.

3.1.3. Discussion. Figure 2c shows the same experimental data as those presented in Figure 2a but plotted in the pressure−temperature plane. Pure CO_2 and pure CH_4 hydrate liquid−hydrate−vapor (L−H−V) equilibrium curves are also presented in this graph, together with the CO_2−CH_4 hydrate equilibrium curve calculated with the empirical correlation proposed by Adisasmito et al.[36] for the gas phase composition measured at point F. This representation is very useful to analyze how the system behaves from a thermodynamic point of view. From the beginning (point A) to the end (point I) of the experiment, the experimental data follow a characteristic loop usually named a "hysteresis curve".

On the one hand, the first solid formed in the bulk at point B crystallizes significantly outside the hydrate stability zone of pure CO_2 and pure CH_4 hydrates. The exothermicity of the first sII hydrate crystallization is hardly detectable in the main plot of Figure 2c, but the small temperature peak obtained is clearly visible in the small inset presented inside this figure. On the other hand, THF is well known to be a strong thermodynamic promoter even at low dosage,[37] and this compound is able to form with pure CO_2 and pure CH_4 mixed THF + CO_2 hydrates[31] and mixed THF + CH_4 hydrates,[38] respectively. These mixed hydrates are of structure sII. Therefore, this crystallization can be attributed unambiguously to a mixed hydrate of structure sII containing THF and a mixture of CO_2 and CH_4. However, it was not possible to quantify precisely the amount and the proportion of CO_2 and CH_4 removed by the formation of this mixed hydrate for two reasons: (i) the reactor is still cooling when this first crystallization occurs and (ii) as the concentration of THF is low (only 4.0 wt %), the quantity of removed gas associated with the sII hydrate crystallization is small and is thus hardly quantifiable with gas chromatographic analyses.

In the absence of THF, the CO_2 + CH_4 guest combination is known to form binary hydrates of structure sI, even though a thermodynamically unstable structure sII can be observed transiently in certain conditions.[39] In Figure 2c, it is important to remark that the pressure reached by the system at the end of the reaction (at point F) matches the equilibrium pressure of the CO_2 − CH_4 binary hydrate calculated by using the empirical correlation proposed by Adisasmito et al.[36] with y^{CO_2} = 67.7 mol % (composition of the gas phase obtained at point F), and is also in agreement with the data obtained using the CSMGem program developed by Sloan and Koh.[7] Therefore, it can be concluded that the second crystallization which starts at point C is very likely to be that of the sI binary CO_2 − CH_4 hydrate.

Regarding the snapshots of Figure 2 in the time interval from point C to point F, interesting morphological changes of the solid formed are observed: dark efflorescences begin to appear from point D and grow progressively in the whole solid visible through the reactor windows. This observation is concomitant

with the high rate gas consumption measured during the experiment. Similar morphologies have already been observed by others,[40] who proposed (on the basis of Raman measure ments) that the difference between clear and dark crystals may be (i) linked to incorporation of free gas and/or free water in the hydrate structure or (ii) due to the transient formation of "fragile solids in a pre hydrate state".

One of the most interesting feature is, as shown in Figure 2c, that this second crystallization formation starts shortly after the hydrate equilibrium line of the binary sI hydrate is crossed. It is likely that, in the case of the two additives used in combination, the formation of the mixed sII hydrate (which forms first) triggers the formation of the latter binary sI hydrate. This conclusion is in agreement with the results obtained in other studies carried out using CO_2 and THF,[34] or CO_2 and cyclopentane,[41] or CH_4 and propane,[42] or CH_4 and THF.[38]

3.2. Influence of SDS and/or THF. This section presents how the presence and the concentration of the two additives tested in this study (THF and SDS) affect the gas separation process, in terms of kinetics and selectivity.

3.2.1. Necessity To Combine the Two Additives. Figure 3 shows the evolution of the reactor pressure and temperature as

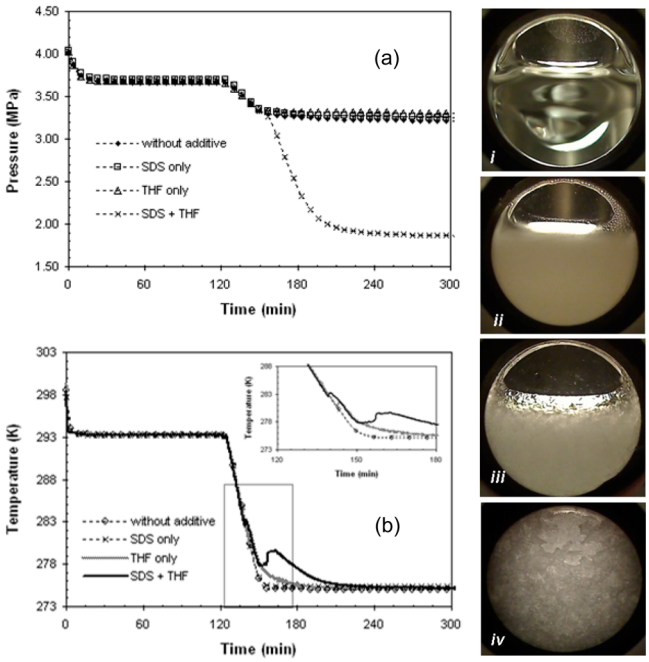

Figure 3. Evolution of the (a) reactor pressure and (b) temperature versus time, obtained with or without using additive(s). Snapshots are taken at time = 300 min. Conditions: [SDS] = 3000 ppm, [THF] = 4.0 wt %, T_{targ} = 275 K, and P_{load} = 4.00 MPa.

a function of time, together with snapshots taken through the reactor window at the end of the experiments. The four cases presented are (i) pure water, (ii) pure water with 3000 ppm SDS, (iii) pure water with 4.0 wt % THF, and (iv) pure water with 3000 ppm SDS and 4.0 wt % THF. The protocol is the same as that described in section 3.1 (T_{targ} = 275 K and P_{load} = 4.00 MPa). Under these conditions, Figure 4 shows precisely the quantity of gas removed and the selectivity of the separation calculated with eqs 1 and 2, respectively.

(i) When only water is used (without any additive), the solution remains transparent (Figure 3, snapshot i) and no

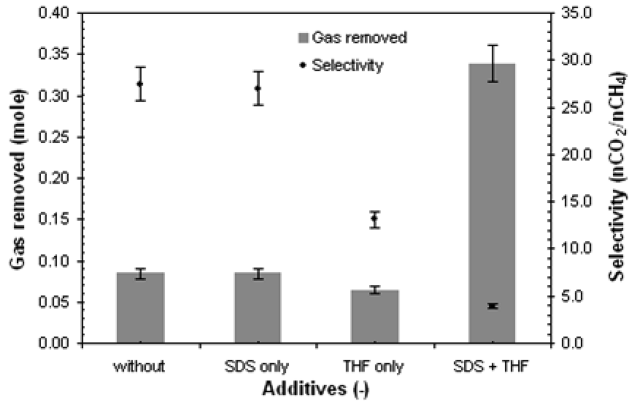

Figure 4. Quantity of gas removed and selectivity of the separation with or without additive(s). Additive concentrations are [SDS] = 3000 ppm and [THF] = 4.0 wt % ; operating conditions are T_{targ} = 275 K and P_{load} = 4.00 MPa.

hydrate crystallization is observed even if the experiment is left for 24 h at 275 K.

(ii) If only SDS is added to the water, the solubility equilibrium is reached slightly more quickly than in the absence of SDS: it is hardly visible in Figure 3b but was clearly shown in our previous results.[35] As the final reactor pressure obtained is the same as with pure water, this means that the addition of this surfactant at the concentration used here has only a kinetic effect. However, we have always observed at 275 K a crystallization of white particles (Figure 3, snapshot ii) without any gas consumption (Figure 3a) and exothermal event (Figure 3b), meaning that the solid formed is not a hydrate. We have performed in parallel studies of the temperature below which there is precipitation of the surfactant (named the "saturation temperature") used at the concentration of 3000 ppm, which in the ambient conditions is slightly above its critical micellar concentration (2300 ppm[43]). These studies are reported in the Appendix. Our results show a SDS saturation temperature equal to T_s = 289 ± 1 K in the absence of THF, in agreement with the value of 285 ± 4 K proposed by Watanabe et al.[44] Interestingly, the saturation temperature of SDS is found to decrease when THF concentration increases (T_s = 280 ± 1 K for 4.0 wt % THF). Therefore, the crystallization observed with the solution containing only SDS is attributed unambiguously to SDS precipitation. As shown in Figure 4, the quantity of gas removed ($n_{removed}$ ~ 0.08 mol) and the value of the selectivity (S ~ 28 mol of CO_2/mol of CH_4) when only SDS is present are of the same order of magnitude as for pure water; confirming that SDS has only a small kinetic effect on solubilization. This high value of selectivity is consistent with the fact that, at 275 K, the solubility of CO_2 is 25−30 times higher than that of CH_4.[45]

(iii) The experiment performed with only THF added to the water shows (see Figure 3) a crystallization at the temperature of 281 K and pressure of 3.44 MPa, together with a small temperature peak but without any gas consumption. This high value of the crystallization temperature is not compatible with the formation of pure THF hydrate,[37] and is very likely to correspond to the formation of (CO_2 and/or CH_4) + THF mixed hydrate. The final pressure level obtained is slightly higher than that obtained with pure water and water + SDS. In this case, we have observed a white solid phase, relatively compact in the whole bulk, visible on snapshot iii presented in Figure 3.

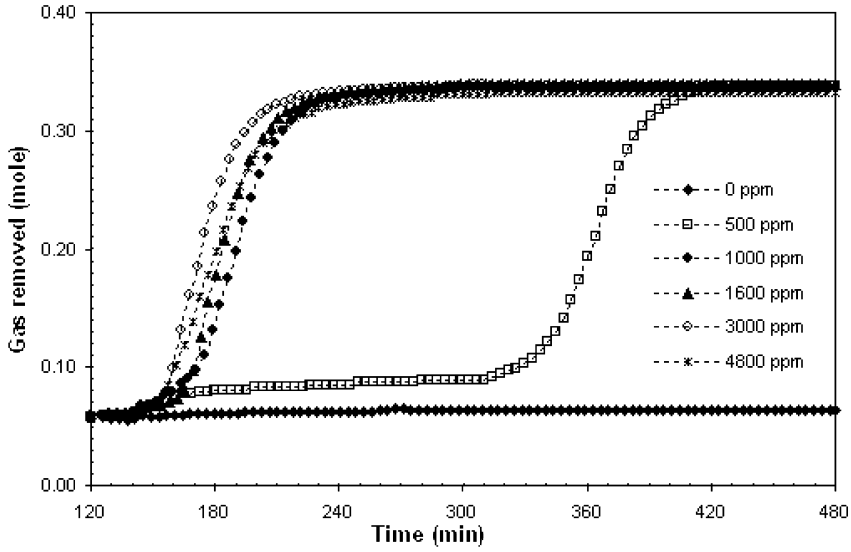

Figure 5. Evolution of the quantity of gas removed versus time for different concentrations of SDS. Conditions: [THF] = 4.0 wt %, T_{targ} = 275 K, and P_{load} = 4.00 MPa.

Table 1. Influence of Additive Concentrations (SDS and THF) and Process Operating Conditions P_{load} and T_{targ} on Values of the Reactor Pressure, Gas Composition, Quantity of Gas Removed, Selectivity of the Separation Obtained at the End of the Reaction (Equilibrium), Values of $t_{50\%}$ and $t_{90\%}$, and Maximum Value of the Enclathration Rate (dn/dt)

				equilibrium conditioins							
						gas removed					
P_{load} (MPa)	T_{targ} (K)	[SDS] (ppm)	[THF] (wt %)	press. (MPa)	y_{CO_2} (mol %)	mol	%	selectivity[a]	$t_{50\%}$ (min)	$t_{90\%}$ (min)	$dn/dt \times 10^{-3}$ (mol/min)
4.00	275	0	4.0	3.30	72.3	0.064	10 6	13.1			
4.00	275	500	4.0	1.82	67.2	0.337	56.4	4.0	356	389	4.563
4.00	275	1000	4.0	1.88	67.1	0.336	55.1	4.1	185	214	5.645
4.00	275	1600	4.0	1.84	67.3	0.340	55.9	4.1	179	207	6.503
4.00	275	3000	4.0	1.86	67.7	0.338	55.5	3.9	169	198	6.572
4.00	275	4800	4.0	1.87	68.2	0.332	54.9	3.8	174	210	5.642
4.00	275	3000	0.0	3.24	71.1	0.084	13.8	27.0			
4.00	275	3000	1.0	1.90	64.7	0.324	54.7	4.6	205	239	4.672
4.00	275	3000	2.0	1.91	66.4	0.328	54.8	4.3	181	217	4.902
4.00	275	3000	4.0	1.86	67.7	0.340	55.5	3.9	169	198	6.572
3.00	275	3000	4.0	1.85	68.5	0.160	37.2	5.2	168	200	2.398
3.50	275	3000	4.0	1.85	67.1	0.225	45.5	4.8	170	201	3.329
4.00	275	3000	4.0	1.86	67.7	0.338	55.5	3.9	169	198	6.572
4.00	275	3000	4.0	1.86	67.7	0.338	55.5	3.9	169	198	6.572
4.00	277	3000	4.0	2.29	69.4	0.268	44.1	4.1	173	226	2.952
4.00	279	3000	4.0	2.87	70.8	0.165	27.2	5.2	172	256	0.752
4.00	281	3000	4.0	3.35	71.6	0.080	13.0	9.9			
4.00	283	3000	4.0	3.35	71.8	0.084	12.8	8.7			

[a] n_{CO_2}/n_{CH_4}.

The formation of the mixed hydrate consumes 17 mol of water/mol of THF trapped, reducing the free water available for gas solubilization. Therefore, a smaller quantity of free water combined with a mixed hydrate which contains certainly some amount of CH_4 leads to a value of selectivity ($S \sim 13$ mol of CO_2/mol of CH_4) lower than the case where pure water, or water + SDS, is used.

(iv) When both SDS and THF additives are used in combination, the behavior observed is drastically different. Two exothermic peaks are observed successively: a peak of small intensity with little gas consumption (similar to that observed when only THF is present), followed by a second larger peak accompanied by a dramatic drop of pressure. In addition, the solidlike morphology is also very different, as shown in snapshot iv of Figure 3, where the structure formed appears granular and contrasted with clear and dark areas. Note that, in this case, a part of the solid always grows up progressively along the reactor window.

Figure 4 compares the different situations (water without additive, with SDS only, with THF only, and with the combination of THF + SDS), in terms of quantity of gas removed and of selectivity of the separation. When no additive is present, the quantity of gas removed and the selectivity are identical to those obtained in the case when only SDS is used.

We have already demonstrated in a previous study[35] that SDS (used at this concentration) does not modify significantly the gas solubility equilibria. Thus, in such cases, no hydrate is formed and the gas removed is only due to the gas solubilization into the solution. When only THF is used, the quantity of gas removed is found to be slightly lower than when no additive or only SDS is used, but remains of the same order of magnitude. However, selectivity decreases due to the capture of CH_4 by the mixed hydrate (CO_2−CH_4 + THF) formed. The system behaves very differently when the two additives are used in combination: the quantity of removed gas ($n_{removed}$ = 0.338 mol) is about 6 times higher than in the three previous cases. In this case, the selectivity of the separation drops to a value close to S = 4 mol of CO_2/mol of CH_4 due to capture of both CO_2 and CH_4 by the hydrates formed. These results clearly indicate that (i) the major quantity of the removed gas is attributed to the formation of the sI binary CO_2−CH_4 hydrate and (ii) this binary hydrate enclathrates more CO_2 than CH_4 but contains a nonnegligible quantity of CH_4.

3.2.2. Effect of Additive Concentration. The effect of surfactant concentration (SDS) on the rate of gas consumption is shown in Figure 5. Note that, for the sake of clarity, the part of the curve concerning the solubilization of CO_2 in the water phase has been omitted. For this set of experiments, THF concentration has been maintained at 4.0 wt %. The results with the quantitative data are presented in Table 1.

As shown previously in Figure 3, in the absence of SDS, gas enclathration does not occur despite the first formation of the mixed hydrate containing THF. When both additives are used in combination, the total quantity of gas removed is independent of SDS concentration in the range 500−4800 ppm, as well as the equilibrium pressure reached by the system at the end of the experiment (see Table 1). However, for the lowest SDS concentration tested (500 ppm), the high rate gas enclathration is dramatically delayed compared to the higher SDS concentrations, as shown graphically in Figure 5 and quantified more precisely by the values of $t_{50\%}$ and $t_{90\%}$ presented in Table 1. For SDS concentrations greater than or equal to 1000 ppm, the gas enclathration rate (dn/dt) and the selectivity (S) are rather insensitive to concentration. Interestingly, the value of the enclathration goes through a slight maximum, and $t_{50\%}$ and $t_{90\%}$ are minimal for a SDS concentration of 3000 ppm. The enclathration rate is found to slightly decrease at the highest SDS concentration tested (4800 ppm).

Figure 6a shows that, in the absence of THF, hydrate formation does not occur (see also section 3.2.1 and Figure 3) and that the quantity of gas consumed is much higher in the presence of THF. Together with the values of $t_{50\%}$ and $t_{90\%}$ presented in Table 1, Figure 6a shows that the enclathration kinetics is also dependent on THF concentration. The value of the gas enclathration rate increases with THF concentration, e.g., dn/dt obtained with 4.0 wt % THF is about 40% higher than the value obtained with 1.0 wt % THF, while the selectivity decreases when THF concentration increases. In addition, due to the thermodynamic promoting effect of THF, it is worth noting that the beginning of the crystallization is delayed when THF concentration decreases. Interestingly, the pressure reached by the system at the end of the experiment is independent of THF concentration in the range of concen trations tested in this study (from 1.0 to 4.0 wt % THF). The final pressure perfectly matches with the L−H−V equilibrium pressure of the sI CO_2−CH_4 hydrate calculated using

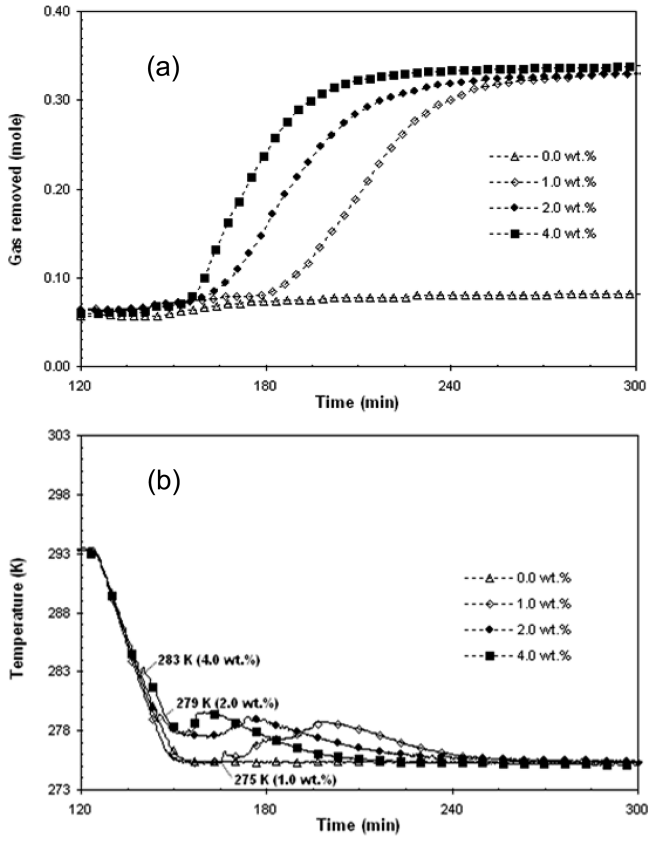

Figure 6. Evolution of the (a) quantity of gas removed and (b) reactor temperature versus time for different concentrations of THF. Conditions: [SDS] = 3000 ppm, T_{targ} = 275 K, and P_{load} = 4.00 MPa.

Adisasmito's correlation[36] with the composition of the remaining gas. In addition, the amplitude and the surface of the temperature peaks measured during the experiments (indicated in Figure 6b at 275, 279, and 283 K for 1, 2, and 4 wt % THF, respectively) show that the quantity of mixed hydrate generated at the first crystallization is correlated with the quantity of THF introduced: the more THF is introduced, the more mixed hydrates are formed. Finally, selectivity is found to decrease with increasing THF concentration, linked to the increase of the remaining free water (where CO_2 is soluble) when THF concentration decreases.

3.2.3. Discussion and Proposal of Action Mechanisms. The results discussed in section 3.2.2 show clearly that the two additives play very important and different roles in the gas enclathration process.

In a first step, THF acts as a thermodynamic promoter and allows the formation of a mixed hydrate which contains this additive and both of the gases (CO_2 and CH_4). Owing to the low concentration of THF initially introduced in the solution, only a small fraction of the water is converted to mixed hydrates. When these first hydrate particles are formed in the bulk, SDS begins to play a positive role: very likely, DS^- anions adsorb on the surface of this mixed hydrate, as already shown experimentally on pure THF hydrates[46] and cyclopentane hydrates,[47,48] and thus may confer antiagglomerant properties to those hydrate particles.[49]

In a second step, when the thermodynamic conditions are suitable, the presence of these hydrate particles (formed first in the bulk) promotes the formation of the binary CO_2−CH_4 hydrate. Very likely, DS^- anions also adsorb on this second

hydrate. By preventing (or limiting) the agglomeration of hydrate particles, the surfactant helps form a "porous hydrate open structure" able to pump the water by capillarity. This porosity could enhance the gas/liquid/solid exchanges, and allows obtaining a high water to hydrate conversion even in quiescent conditions. This porous structure, which accumulates principally along the cold reactor walls, is apparent and persists long enough to be visualized (we have distinctly observed it) when the reactor is open at the end of the hydrate formation step.[28,41]

One of the most interesting results is that the gas enclathration rate is dependent on the concentration of the thermodynamic additive, and that this observation cannot be attributed to the thermodynamic effect of THF. With the low THF concentrations used here, it is likely that most of the THF initially introduced is enclathrated instantaneously when the first mixed sII hydrate crystallizes, and thus the residual THF concentration is probably negligible. The increase of dn/dt with THF concentration may be linked to the presence in the bulk of a higher amount of mixed hydrate. The two hydrate structures sII and sI coexisting together in the reactor could influence the global structure of the solid formed and make a whole porous fine grained structure (as already observed in other studies[40]), thus enhancing the enclathration rate.

3.3. Influence of the Process Operating Conditions. This section presents the influence of the process operating conditions, i.e., the gas loading pressure (P_{load}) and the reactor target temperature (T_{targ}), on the quantity of gas removed and on the selectivity of the CO_2/CH_4 separation. On the basis of the conclusions drawn from sections 3.1.3 and 3.2.3, the additive concentrations chosen are 3000 ppm SDS and 4.0 wt % THF, thus maximizing the enclathration rate.

The influence of P_{load} has been investigated for P_{load} = 3.00, 3.50, and 4.00 MPa, with T_{targ} set to 275 K. Figure 7 shows the evolution of the reactor pressure and the gas removed as a function of time for the three experiments, and the results are summarized in Table 1.

Figure 7 and Table 1 show that (i) the pressure drop, the quantity of gas removed, and the gas enclathration rate increase with P_{load}, and (ii) the equilibrium pressure does not depend significantly on P_{load}. When P_{load} increases, the conversion of water into binary $CO_2 - CH_4$ hydrates before reaching the L−H−V equilibrium point also increases, and thus the quantity of gas removed is more important. The increase of water conversion with P_{load} leads to a smaller quantity of remaining free water at the end of the experiment, and therefore the CO_2 fraction in the remaining gas is found to slightly increase and the selectivity of the separation to decrease (or, equivalently, a lesser amount of CO_2 is removed from the gas phase by solubilization in the water phase).

The influence of T_{targ} has been studied for five different temperatures between 275 and 283 K. The evolution of the quantity of gas removed as a function of time is presented in Figure 8a, and the results are summarized in Table 1. For each temperature tested, Figure 8b shows the pressure−temperature diagram drawn with the final $P-T$ conditions obtained at the end of each experiment, superimposed to some relevant hydrate equilibrium curves (i.e., pure CH_4 and pure CO_2 hydrates, mixed CO_2 + THF ([THF] = 4.0 wt %) and CH_4 + THF ([THF] = 4.2 wt %) hydrates). Unfortunately, no equilibrium data have been found in the literature for (CO_2−CH_4) + THF mixed hydrates.

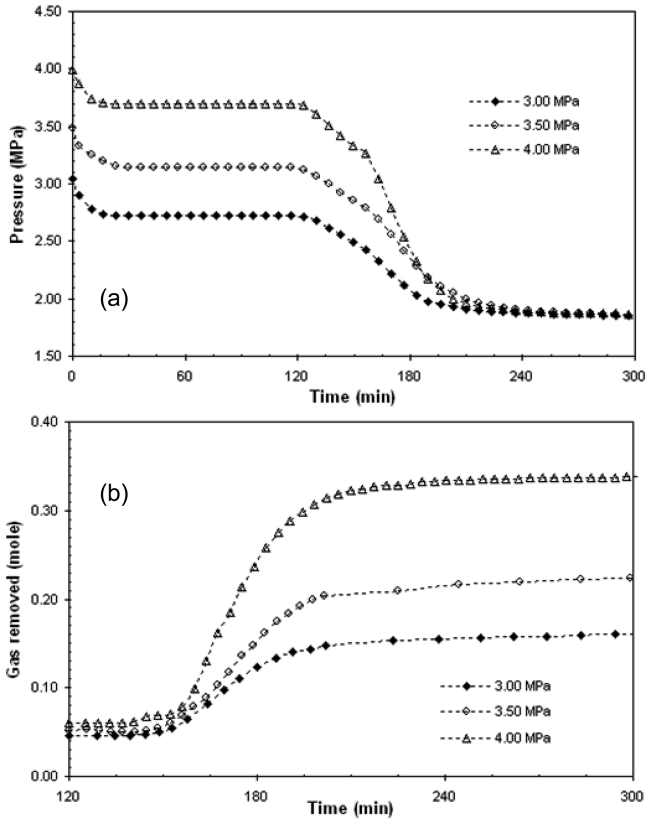

Figure 7. Evolution of the (a) reactor pressure and (b) quantity of gas removed versus time for different gas loading pressures of the reactor (P_{load}). Conditions: [SDS] = 3000 ppm, [THF] = 4.0 wt %, and T_{targ} = 275 K.

The results presented in Table 1 demonstrate clearly that an increase of T_{targ} drastically impacts the quantity of gas removed during the reaction. For example, 55.5% of the initial gas is removed at 275 K while only 27.2% is removed at 279 K. Increasing this temperature has the effect of decreasing significantly the enclathration rate (from 6.572×10^{-3} mol/min at 275 K to 7.540×10^{-4} mol/min at 279 K). However, the selectivity of the separation is found to slightly increase when temperature increases from 275 to 279 K, because there is a higher quantity of remaining free water. Interestingly, for the two highest temperatures tested (281 and 283 K), the quantity of gas removed is low (around 13% of the initial loaded gas), while selectivity is quite high (S = 9.9 mol of CO_2/mol of CH_4 for 281 K and 8.7 mol of CO_2/mol of CH_4 for 283 K). For these two temperatures (281 and 283 K), Figure 8b shows that the final $P-T$ points obtained at the end of the experiments fall outside the region delimited by the pure CO_2 and pure CH_4 hydrate equilibrium curves: as a consequence, the formation of the binary CO_2 + CH_4 hydrate equilibrium is not possible. Oppositely, considering the position of the mixed CO_2 + THF and CH_4 + THF hydrates obtained with a concentration close to 4.0 wt % THF, it is likely that only a mixed hydrate has formed at these temperatures, leading to a larger amount of free water available compared to the experiments carried out a lower temperature and thus a slightly higher selectivity ($S \sim 9$ mol of CO_2/mol of CH_4).

Concerning the two process parameters studied (P_{load} and T_{targ}), a higher initial reactor pressure and a lower target reactor temperature allow obtaining a larger conversion of water into hydrates, and consequently a more important quantity of gas

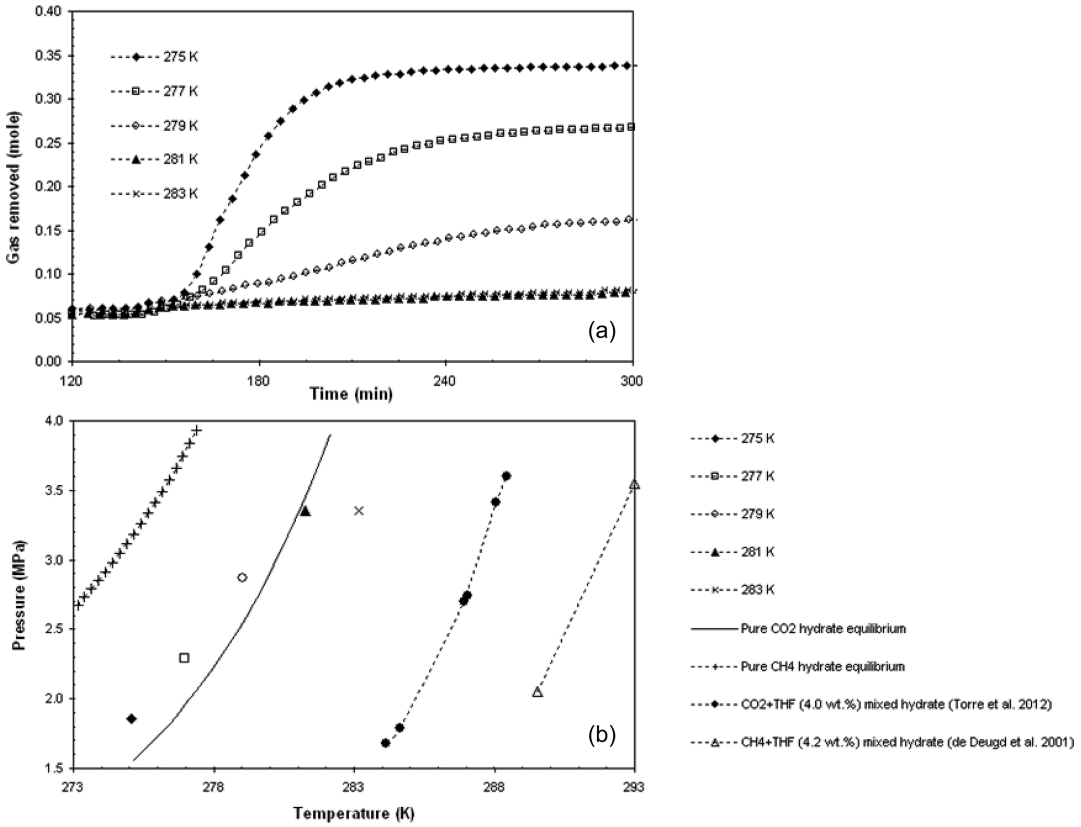

Figure 8. (a) Evolution of the quantity of gas removed versus time ; (b) P−T diagram with reactor pressure data obtained at the end of experiments carried out with different target temperatures (T_{targ}). Conditions: [SDS] = 3000 ppm, [THF] = 4.0 wt %, and P_{load} = 4.00 MPa. Equilibrium curves are those of pure CH_4 and pure CO_2 hydrates (from the CSMGem program[7]), mixed CO_2 + THF hydrate,[34] and mixed CH_4 + THF hydrate.[30]

removed. This result is easily understandable as the conversion is directly correlated, when the reactor is operated in batch conditions, to the *driving force* between the initial operating point (imposed by the operator) and the final equilibrium point (reached by the system). Note that, for a given temperature, the *driving force* is defined as the difference between the reactor pressure and the equilibrium pressure.[50] Concerning the kinetic parameters, the gas enclathration kinetics being directly proportional to the driving force,[51] the increase of P_{load} and the decrease of T_{targ} directly enhance the enclathration rate. Finally, the enclathration process stops when the L−H−V equilibrium (with respect to the gas phase composition) is reached.

3.4. Summary of the Trends Observed. Table 2 highlights and summarizes the trends observed for the three salient parameters of this study, namely, the quantity of gas removed ($n_{removed}$), the selectivity of the separation (S), and the enclathration rate (dn/dt), as a function of the SDS concentration ([SDS]) and THF concentration ([THF]), initial gas loading pressure (P_{load}), and target temperature (T_{targ}) of the reactor.

Interestingly, Table 2 illustrates clearly that, when the reactor is operated in batch mode under the conditions tested in this work, it is not possible to maximize at the same time the three factors ($n_{removed}$, S, and dn/dt) and, accordingly, a trade off has to be found.

Table 2. Summary Table of the Different Trends Observed[a]

	influence on parameters		
increase in variable	$n_{removed}$	S	dn/dt
[SDS]	↔	↔	↑[b]
[THF]	↑	↓	↑
P_{load}	↑	↓	↑
T_{targ}	↓	↑	↓

[a]↑, increasing effect; ↓, decreasing effect; ↔, no effect. [b]Until 3000 ppm.

4. CONCLUSIONS

In this work, we have studied the potentiality of a hydrate based process to separate CO_2 from a CO_2−CH_4 gas mixture (rich in CO_2) in the presence of THF and/or SDS in a batch reactor operated in quiescent conditions. The influence of the additive concentrations and process operating conditions has been investigated with regard to the gas enclathration kinetics, the quantity of gas removed, and the selectivity of the separation.

For the conditions tested in this study, the enclathration of a large quantity of gas in a reasonable time is possible only when SDS and THF are used in combination. When SDS and THF are both present, we propose the following mechanism consistent with our observations, measurements, and thermo dynamic considerations using the available equilibrium data: mixed hydrate containing THF, CO_2, and CH_4 crystallizes first in the form of hydrate particles when the reactor is cooled down, and then these particles trigger the formation of a second binary hydrate containing only CO_2 and CH_4.

SDS concentration plays an important role in the enclathration process: the enclathration rate is found to increase with this concentration, with a maximum obtained in

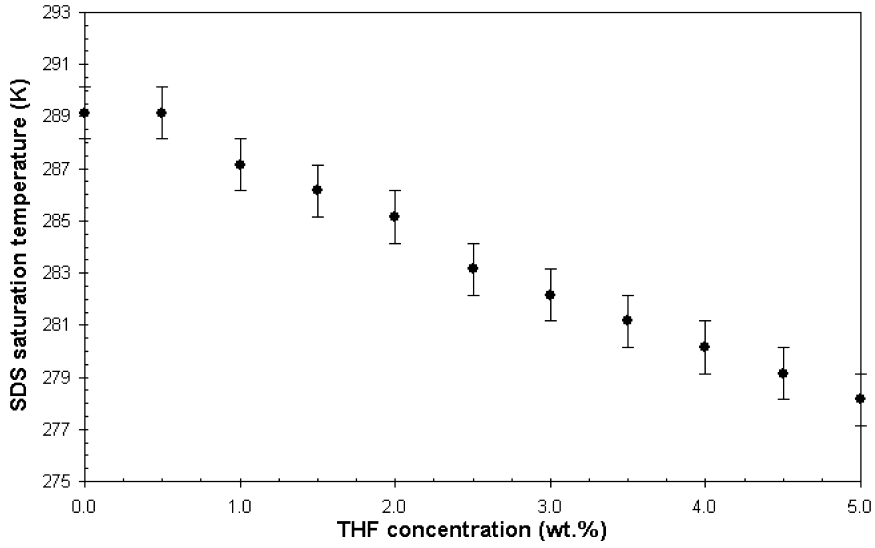

Figure 9. SDS saturation temperature as a function of THF concentration. SDS concentration in the solution is 3000 ppm.

the range 1600−3000 ppm. However, no substantial effect is noted on the quantity of gas removed and on the selectivity of the separation. It is very likely that SDS plays a positive role in limiting hydrate agglomeration, e.g., by adsorption on the hydrate surface, and favors the formation of a porous hydrate structure which grows along the cold reactor walls.

It is clear that THF concentration is directly related to the quantity of mixed hydrate formed first when the reactor is cooled down. This mixed hydrate of unknown composition in CO_2 and CH_4 converts a appreciable quantity of water (17 mol of water/mol of THF). Thus, since water is in excess (the hydrate equilibrium is always reached before consuming all the water available), the increase in THF concentration reduces the quantity of remaining free water at the end of the reaction and, as CO_2 is much more soluble in water than CH_4, leads to an increase of the selectivity of the separation. In addition, we found that the enclathration rate increases with THF concentration. As the THF is supposed to be totally enclathrated in the first mixed hydrate, we believe that the increase of the enclathration rate cannot be attributed to a thermodynamic effect of the THF. This may be linked to the quantity of mixed hydrate initially generated in the bulk, which could have a positive effect on the whole structure of the hydrates formed, e.g., by forming a fined grained porous mass of hydrates due to the coexistence of the two hydrate structures sI and sII. Nevertheless, the assumption such as the THF initially introduced is totally enclathrated by the first mixed hydrate needs confirmation by performing further experiments and in situ analyses.

The influences of operating conditions, i.e., the reactor loading pressure and the reactor target temperature, are of importance. More gas is removed and the enclathration rate is higher if the reactor loading pressure is increased and/or the target temperature is decreased, in accord with the usual *driving force* considerations, owing to that the kinetic performance of the process is more favorable when the operating point is further inside the hydrate stability zone.

Concerning the selectivity of the CO_2 separation, which increases when the reactor temperature target increases and when the loading pressure decreases, this is likely to be linked to the quantity of free water available at the end of the experiment (which is more important when the water to hydrate conversion is reduced). To be closer to a real industrial hydrate based process, additional experiments could be carried out in semi batch reactor mode (where a total conversion of water is reached) to determine more precisely the selectivity due to the hydrate phases only. However, the selectivity of the hydrate based process appears to be not high enough toward CO_2 to foresee such a separation process at the industrial scale for a CO_2−CH_4 gas mixture.

The combination of both a thermodynamic promoter (THF) and a kinetic promoter (SDS) appears very interesting to consider as a possible way to enhance the CO_2 separation by clathrate hydrate formation. However, deep understanding of the possible interactions, and synergism between hydrates and additives, and particularly to clarify the role played by the surfactant, requires performing additional fundamental research investigations.

APPENDIX

The saturation temperature of the SDS, denoted T_s, has been determined for a concentration equal to 3000 ppm. Different concentrations of THF (from 0.0 to 5.0 wt %) in water have been considered for this study. Glass tubes, filled with 10 cm^3 of solution containing the additive(s) and closed hermetically, are plunged in a thermostatic bath where the temperature is regulated initially at 274 K. This temperature is increased by steps of 1 K per day, and visual observations are carried out each day. The saturation temperature is defined as the temperature where the precipitate is no longer visible with the naked eye. The precision of the measurement is evaluated to be equal to ±1 K. The results obtained are presented in Figure 9.

AUTHOR INFORMATION

Corresponding Author

*Tel.: +33(0)5 40 17 51 09. Fax: +33(0)5 79 40 77 25. E mail: jean philippe.torre@univ pau.fr.

Notes

The authors declare no competing financial interest.

■ ACKNOWLEDGMENTS

The authors would like to thank J. Diaz for his valuable assistance on the pilot rig. Fundayacucho from Venezuela, Total E&P ("Gas Solutions" R&D Project) and CG64 (Conseil Général des Pyrénées Atlantiques), are gratefully acknowledged for financial support of this work.

■ REFERENCES

(1) BP. *Statistical Review of World Energy 2010*; BP: London, U.K., 2010. www.bp.com/statisticalreview.

(2) Economides, M. J.; Oligney, R. E.; Lewis, P. E. U.S. Natural Gas in 2011 and Beyond. *J. Nat. Gas Sci. Eng.* **2012**, *8*, 2−8.

(3) Bellussi, G.; Broccia, P.; Carati, A.; Millini, R.; Pollesel, P.; Rizzo, C.; Tagliabue, M. Silica−aluminas for Carbon Dioxide Bulk Removal from Sour Natural Gas. *Microporous Mesoporous Mater.* **2011**, *146* (1−3), 134−140.

(4) Rufford, T. E.; Smart, S.; Watson, G. C. Y.; Graham, B. F.; Boxall, J.; Diniz da Costa, J. C.; May, E. F. The Removal of CO_2 and N_2 from Natural Gas: a Review of Conventional and Emerging Process Technologies. *J. Pet. Sci. Eng.* **2012**, *94*−*95*, 123−154.

(5) Yeo, Z. Y.; Chew, T. L.; Zhu, P. W.; Mohamed, A. R.; Chai, S. P. Conventional Processes and Membrane Technology for Carbon Dioxide Removal from Natural Gas: A Review. *J. Nat. Gas Chem.* **2012**, *21*, 282−298.

(6) Kohl, A. L.; Nielsen, R. B. *Gas Purification*, 5th ed.; Gulf Publishing Co.: Houston, TX, 1997.

(7) Sloan, E. D.; Koh, C. A. *Clathrate Hydrates of Natural Gases*, 3rd ed.; CRC Press, Taylor & Francis: New York, 2008.

(8) Sloan, E. D. Fundamental Principles and Applications of Natural Gas Hydrates. *Nature* **2003**, *426* (20), 353−359.

(9) Sum, A. K.; Koh, C. A.; Sloan, E. D. Clathrate Hydrates: from Laboratory Science to Engineering Practice. *Ind. Eng. Chem. Res.* **2009**, *48*, 7457−7465.

(10) Zerpa, L. E.; Salager, J. L.; Koh, C. A.; Sloan, E. D.; Sum, A. K. Surface Chemistry and Gas Hydrates in Flow Assurance. *Ind. Eng. Chem. Res.* **2011**, *50*, 188−197.

(11) Sun, C.; Li, W.; Yang, X.; Li, F.; Yuan, Q.; Mu, L.; Chen, J.; Liu, B.; Chen, G. Progress in Research of Gas Hydrate. *Chin. J. Chem. Eng.* **2011**, *19* (1), 151−162.

(12) Eslamimanesh, A.; Mohammadi, A. H.; Richon, D.; Naidoo, P.; Ramjugernath, D. Application of gas hydrate formation in separation processes: A review of experimental studies. *J. Chem. Thermodyn.* **2012**, *46*, 62−71.

(13) Kuramochi, T.; Ramírez, A.; Turkenburg, W.; Faaij, A. Techno economic Assessment and Comparison of CO_2 Capture Technologies for Industrial Processes: Preliminary Results for the Iron and Steel Sector. *Energy Procedia* **2011**, *4*, 1981−1988.

(14) Mondal, M. K.; Balsora, H. K.; Varshney, P. Progress and Trends in CO_2 Capture/Separation Technologies: A Review. *Energy* **2012**, *46*, 431−441, DOI: 10.1016/j.energy.2012.08.006.

(15) Duc, N. H.; Chauvy, F.; Herri, J. M. CO_2 Capture by Hydrate Crystallization—A Potential Solution for Gas Emission of Steelmaking Industry. *Energy Convers. Manage.* **2007**, *48*, 1313−1322.

(16) Seo, Y. T.; Kang, S. P.; Lee, H.; Lee, C. S.; Sung, W. M. Hydrate Phase Equilibria for Gas Mixtures Containing Carbon Dioxide: a Proof of concept to Carbon Dioxide Recovery from Multicomponent Gas Stream. *Korean J. Chem. Eng.* **2000**, *17* (6), 659−667.

(17) Seo, Y. T; Lee, H. Hydrate Phase Equilibria of the Carbon Dioxide, Methane and Water System. *J. Chem. Eng. Data* **2001**, *46*, 381−384.

(18) van Denderen, M.; Ineke, E.; Golombok, M. CO_2 Removal from Contaminated Natural Gas Mixtures by Hydrate Formation. *Ind. Eng. Chem. Res.* **2009**, *48*, 5802−5807.

(19) Herri, J. M.; Bouchemoua, A.; Kwaterski, M.; Fezoua, A.; Ouabbas, Y.; Cameirao, A. Gas Hydrate Equilibria for CO_2 N_2 and CO_2 CH_4 Gas Mixtures—Experimental Studies and Thermodynamic Modelling. *Fluid Phase Equilib.* **2011**, *301*, 171−190.

(20) Golombok, M.; Ineke, E.; Rojas, J. C.; He, Y. Y.; Zitha, P. Resolving CO_2 and Methane Hydrate Formation Kinetics. *Environ. Chem. Lett.* **2009**, *7*, 325−330.

(21) Herri, J. M.; Kwaterski, M. Derivation of a Langmuir Type of Model to Describe the Intrinsic Growth Rate of Gas Hydrates During Crystallization from Gas Mixtures. *Chem. Eng. Sci.* **2012**, *81*, 28−37.

(22) Okutani, K.; Kuwabara, Y.; Mori, Y. H. Surfactant Effects on Hydrate Formation in an Unstirred Gas/liquid System: An Experimental Study Using Methane and Sodium Alkyl Sulfates. *Chem. Eng. Sci.* **2008**, *63*, 183−194.

(23) Seo, Y. T.; Kang, S. P.; Lee, H. Experimental Determination and Thermodynamic Modeling of Methane and Nitrogen Hydrates in the Presence of THF, Propylene Oxide, 1,4 dioxane and Acetone. *Fluid Phase Equilib.* **2001**, *189*, 99−110.

(24) Karaaslan, U.; Parlaktuna, M. Promotion Effect of Polymers and Surfactants on Hydrate Formation Rate. *Energy Fuels* **2002**, *16* (6), 1413−1416.

(25) Li, S.; Fan, S.; Wang, J.; Lang, X.; Wang, Y. Semiclathrate Hydrate Phase Equilibria for CO_2 in the Presence of Tetra n butyl Ammonium Halide (Bromide, Chloride, or Fluoride). *J. Chem. Eng. Data* **2010**, *55* (9), 3212−3215.

(26) Karanjkar, P. U.; Lee, J. W.; Morris, J. F. Surfactant Effects on Hydrate Crystallization at the Water−Oil Interface: Hollow Conical Crystals. *Cryst. Growth Des.* **2012**, *12* (8), 3817−3824.

(27) Verrett, J.; Posteraro, D.; Servio, P. Surfactant Effects on Methane Solubility and Mole Fraction during Hydrate Growth. *Chem. Eng. Sci.* **2012**, *84*, 80−84.

(28) Gayet, P.; Dicharry, C.; Marion, G.; Graciaa, A.; Lachaise, J.; Nesterov, A. Experimental Determination of Methane Hydrate Dissociation Curve up to 55 MPa by Using a Small Amount of Surfactant as Hydrate Promoter. *Chem. Eng. Sci.* **2005**, *60*, 5751−5758.

(29) Kalogerakis, N.; Jamaluddin, A. K. M.; Dholabhai, P. D.; Bishnoi, P. R. Effect of Surfactants on Hydrate Formation Kinetics. *Proceedings of SPE Internation Sympsoium on Oilfield Chemistry, New Orleans, LA*; Society of Petroleum Engineers: Allen, TX, 1993; SPE 25188.

(30) de Deugd, R. M.; Jager, M. D.; de Swaan, J. Mixed Hydrates of Methane and Water soluble Hydrocarbons Modeling of Empirical Results. *AIChE J.* **2001**, *47* (3), 693−704.

(31) Shin, H. J.; Lee, Y. J.; Im, J. H.; Han, K. W.; Lee, J. W.; Lee, Y.; Lee, J. D.; Jang, W. Y.; Yoon, J. H. Thermodynamic Stability, Spectroscopic Identification and Cage Occupation of Binary CO_2 Clathrate Hydrates. *Chem. Eng. Sci.* **2009**, *64*, 5125−5130.

(32) Lee, H. J.; Lee, J. D.; Linga, P.; Englezos, P.; Kim, Y. S.; Lee, M. S.; Kim, Y. D. Gas Hydrate Formation Process for Pre combustion Capture of Carbon Dioxide. *Energy* **2010**, *35*, 2729−2733.

(33) Torré, J. P.; Dicharry, C.; Ricaurte, M.; Daniel David, D.; Broseta, D. CO_2 Capture by Hydrate Formation in Quiescent Conditions: in Search of Efficient Kinetic Additives. *Energy Procedia* **2011**, *4(C)*, 621−628.

(34) Torré, J. P.; Ricaurte, M.; Dicharry, C.; Broseta, D. CO_2 Enclathration in the Presence of Water soluble Hydrate Promoters: Hydrate Phase Equilibria and Kinetic Studies in Quiescent Conditions. *Chem. Eng. Sci.* **2012**, *82*, 1−13.

(35) Ricaurte, M.; Torré, J. P.; Asbai, A.; Broseta, D.; Dicharry, C. Experimental Data, Modeling, and Correlation of Carbon Dioxide Solubility in Aqueous Solutions Containing Low Concentrations of Clathrate Hydrate Promoters: Application to CO_2−CH_4 Gas Mixtures. *Ind. Eng. Chem. Res.* **2012**, *51* (7), 3157−3169.

(36) Adisasmito, S.; Frank, R. J.; Sloan, E. D. Hydrates of Carbon Dioxide and Methane Mixtures. *J. Chem. Eng. Data* **1991**, *36*, 68−71.

(37) Delahaye, A.; Fournaison, L.; Marinhas, S.; Chatti, I.; Petitet, J. P.; Dalmazzone, D.; Fürst, W. Effect of THF on Equilibrium Pressure and Dissociation Enthalpy of CO_2 Hydrates Applied to Secondary Refrigeration. *Ind. Eng. Chem. Res.* **2006**, *45*, 391−397.

(38) Seo, Y. T.; Lee, H.; Moudrakovski, I.; Ripmeester, J. A. Phase Behavior and Structural Characterization of Coexisting Pure and Mixed Clathrate Hydrates. *ChemPhysChem* **2003**, *4*, 379−382.

(39) Staykova, D. K.; Kuhs, W. F.; Salamatin, A. N.; Hansen, T. Formation of Porous Gas Hydrates from Ice Powders: Diffraction Experiments and Multistage Model. *J. Phys. Chem. B* **2003**, *107* (37), 10299−10311.
(40) Schicks, J. M.; Naumann, R.; Erzinger, J.; Hester, K. C.; Koh, C. A.; Sloan, E. D. Phase Transitions in Mixed Gas Hydrates: Experimental Observations versus Calculated Data. *J. Phys. Chem. B* **2006**, *110* (23), 11468−11474.
(41) Zhang, J.; Lee, J. W. Enhanced Kinetics of CO_2 Hydrate Formation under Static Conditions. *Ind. Eng. Chem. Res.* **2009**, *48*, 5934−5942.
(42) Uchida, T.; Moriwaki, M.; Takeya, S.; Ikeda, I.; Ohmura, R.; Nagao, J.; Minagawa, H.; Ebinuma, T.; Narita, H.; Gohara, K.; Mae, S. Two Step Formation of Methane Propane Mixed Gas Hydrates in a Batch Type Reactor. *AIChE J.* **2004**, *50* (2), 518−523.
(43) Rana, D.; Neale, G. H.; Hornof, V. Surface Tension of Mixed Surfactant Systems: Lignosulfonate and Sodium Dodecyl Sulfate. *Colloid Polym. Sci.* **2002**, *280*, 775−778.
(44) Watanabe, K.; Imai, S.; Mori, Y. H. Surfactant Effects on Hydrate Formation in an Unstirred Gas/liquid System: an Experimental Study Using HFC 32 and Sodium Dodecyl Sulphate. *Chem. Eng. Sci.* **2005**, *60*, 4846−4857.
(45) Qin, J.; Rosenbauer, R. J.; Duan, Z. Experimental Measurements of Vapor−Liquid Equilibria of the $H_2O + CO_2 + CH_4$ Ternary System. *J. Chem. Eng. Data* **2008**, *53*, 1246−1249.
(46) Zhang, J. S.; Lo, C.; Somasundaran, P.; Lu, S.; Couzis, A.; Lee, J. W. Adsorption of Sodium Dodecyl Sulfate at THF Hydrate/Liquid Interface. *J. Phys. Chem. C* **2008**, *112* (32), 12381−12385.
(47) Salako, O.; Lo, C.; Zhang, J. S.; Couzis, A.; Somasundaran, P.; Lee, J. W. Adsorption of Sodium Dodecyl Sulfate onto Clathrate Hydrates in the Presence of Salt. *J. Colloid Interface Sci.* **2012**, *386* (1), 333−337.
(48) Lo, C.; Zhang, J. S.; Couzis, A.; Somasundaran, P.; Lee, J. W. Adsorption of Cationic and Anionic Surfactants on Cyclopentane Hydrates. *J. Phys. Chem. C* **2010**, *114*, 13385−13389.
(49) Anklam, M. R.; York, J. D.; Helmerich, L.; Firoozabadi, A. Effects of Antiagglomerants on the Interactions Between Hydrate Particles. *AIChE J.* **2008**, *54*, 565−574.
(50) Kashchiev, D.; Firoozabadi, A. Driving Force for Crystallization of Gas Hydrates. *J. Cryst. Growth* **2007**, *241*, 220−230.
(51) Ribeiro, C. P., Jr.; Lage, P. L. C.. Modelling of Hydrate Formation Kinetics: State of the art and Future Directions. *Chem. Eng. Sci.* **2008**, *63*, 2007−2034.